

Gene expression profiling in vLINCL CLN6-deficient fibroblasts: Insights into pathobiology

C.A.F. Teixeira^{a,c,d}, S. Lin^b, M. Mangas^{a,d}, R. Quinta^{a,d}, C.J.P. Bessa^{a,d}, C. Ferreira^a,
M.C. Sá Miranda^d, R-M.N. Boustany^c, M.G. Ribeiro^{a,*}

^a Unidade de Enzimologia, Instituto de Genética Médica Jacinto Magalhães, Porto, Portugal

^b Duke Bioinformatics Shared Resource, Duke University Medical Center, Medical Science Research Building, Durham, NC 27710, USA

^c Departments of Pediatrics and Neurobiology, Duke University Medical Center, Medical Science Research Building, Durham, NC 27710, USA

^d Unidade da Biologia do Lisossoma e Peroxissoma do Instituto de Biologia Molecular e Celular da Universidade do Porto, Portugal

Received 22 September 2005; received in revised form 31 May 2006; accepted 1 June 2006

Available online 8 June 2006

Abstract

The CLN6 vLINCL is caused by molecular defects in CLN6 gene coding for an ER resident transmembrane protein whose function is unknown. In the present study gene expression profiling of CLN6-deficient fibroblasts using cDNA microarray was undertaken in order to provide novel insights into the molecular mechanisms underlying this neurodegenerative fatal disease. Data were validated by qRT-PCR. Statistically significant alterations of expression were observed for 12 transcripts. The two most overexpressed genes, versican and tissue factor pathway inhibitor 2, are related to extracellular matrix (ECM), predicting changes in ECM-related proteins in CLN6-deficient cells. Transcript profiling also suggested alterations in signal transduction pathways, apoptosis and the immune/inflammatory response. Up-regulated genes related to steroidogenesis or signalling, and the relationship between cholesterol dynamics and glycosphingolipid sorting, led to investigation of free cholesterol and gangliosides in CLN6-deficient fibroblasts. Cholesterol accumulation in lysosomes suggests a homeostasis block as a result of CLN6p deficiency. The cholesterol imbalance may affect structure/function of caveolae and lipid rafts, disrupting signalling transduction pathways and sorting cell mechanisms. Alterations in protein/lipid intracellular trafficking would affect the composition and function of endocytic compartments, including lysosomes. Dysfunctional endosomal/lysosomal vesicles may act as one of the triggers for apoptosis and cell death, and for a secondary protective inflammatory response. In conclusion, the data reported provide novel clues into molecular pathophysiological mechanisms of CLN6-deficiency, and may also help in developing disease biomarkers and therapies for this and other neurodegenerative diseases. © 2006 Elsevier B.V. All rights reserved.

Keywords: Neuronal Ceroid Lipofuscinoses; CLN6; Genechip analysis; qRT-PCR analysis; Cholesterol

Abbreviations: AKR1C3 (3 α -HSD), aldo-keto reductase family I, member C3 (3- α -hydroxysteroid dehydrogenase, type II); BCHE, butyrylcholinesterase; CAV2, caveolin 2; CNS, central nervous system; CSPG2, chondroitin sulphate proteoglycan 2 (versican); C1R, complement component 1, r subcomponent; ECM, extracellular matrix; ER, endoplasmic reticulum; ERGIC, endoplasmic reticulum Golgi intermediate compartment; GAPDH, glyceraldehyde-3-phosphate dehydrogenase; GARP, glycoprotein A repetitions predominant; HSPA1B7 (HSP70-2), Human HMC class III heat shock HSP70-2 gene (HLA), 70 kDa protein 1B; INCL, infantile NCL; JNCL, juvenile NCL; LDL, low-density lipoprotein; LINCL, late-infantile NCL; LOXL2, lysyl oxidase-like 2; MATP, membrane-associated transporter protein (AIM1, melanoma antigen AIM1/human non-lens beta gamma-crystallin like complex); NCL, neuronal ceroid lipofuscinosis; PP5, placental protein 5; QPCT, glutaminyl-peptide cyclotransferase (glutaminyl cyclase); qRT-PCR, quantitative real-time PCR; RAP1, GTP-GDP dissociation stimulator 1; RRAS2, Ras-like protein TC21; RTVP1, Glioma pathogenesis-related protein (RTVP-1 protein); TFPI-2, tissue factor pathway inhibitor 2; TRPM2/CLU, Testosterone-repressed message 2 (clusterin, complement lysis inhibitor, SP-40, sulfated glycoprotein 2, apolipoprotein J); vLINCL, variant late-infantile NCL

* Corresponding author. Unidade de Enzimologia, Instituto de Genética Médica Jacinto Magalhães, Pç. Pedro Nunes no. 88, 4050-466 Porto, Portugal. Tel.: +351 226070300; fax: +351 226070399.

E-mail address: gil.ribeiro@igm.min-saude.pt (M.G. Ribeiro).

0925-4439/\$ - see front matter © 2006 Elsevier B.V. All rights reserved.

doi:10.1016/j.bbadis.2006.06.002

1. Introduction

The neuronal ceroid-lipofuscinoses (NCL) are a group of autosomal recessive neurodegenerative diseases with an incidence ranging from 0.1 to 7 per 100,000 live births. Clinical features include visual failure, seizures, progressive mental and motor deterioration, and premature death. There is accumulation of autofluorescent lipofuscin-like material in the lysosomes of neurons and other cell types. Three classical subtypes (infantile, late-infantile and juvenile) are described based on age of onset, clinical course and the ultrastructural appearance of membrane-bound inclusions. Presently, six genetically distinct types are recognized [1].

Classical infantile, late-infantile and juvenile are caused by mutations in CLN1, CLN2 and CLN3 genes, respectively. CLN1p/PPT1 and CLN2p/TPP1 are soluble lysosomal enzymes, whereas CLN3 is an intrinsic membrane protein. Variant late-infantile phenotype (vLINCL) exhibits subtle, but distinct clinical and histological differences from classical LINCL. The age of onset may be as late as 6 years of age, with death occurring between the age of 13 and 30 years. In the vast majority of cases inclusion bodies consist of a mix of curvilinear and fingerprint-like bodies. vLINCL phenotype arises from mutations in CLN5, CLN6 or CLN8 coding for proteins with predicted membrane topology [2]. Primary lysosomal dysfunction in NCL is only evident for CLN1 and CLN2.

The CLN6 gene was cloned in 2002 [3,4] and unlike other NCLs no prevalent mutation has been identified. A total of 22 mutations distributed across the entire coding region have been described [5,6], and they were found in ethnic groups from different countries (Argentina, Costa Rica, Portugal, Greece, Italy, India, Morocco, Pakistan, Turkey, Venezuela, North America and Sudan). The gene encodes a 311 amino-acid protein with seven putative transmembrane domains whose topology is not yet known. Recent data suggests that CLN6p, 27–30 kDa, is an ER-resident protein [7,8]. CLN8p is also an ER protein and may recycle between ER and ERGIC [9]. As a member of the eukaryotic family of TLC (TRAM-Lag1p-CLN8)-domain homologues [10] CLN8p may act as a sterol-sensing-domain protein or intracellular chaperone and/or have a role in biosynthesis or transport of lipid molecules.

In the present study global gene expression was analyzed in CLN6-deficient human fibroblasts in order to gain insight into the pathophysiological mechanisms operating in the disease. The altered expression pattern generated by cDNA microarray and confirmed by qRT-PCR suggests that changes in ECM architecture and signalling are likely to be involved in development and progression of disease. Expression of genes involved in stress/apoptosis and in immune/inflammatory responses was also altered, supporting the notion that these may be important for neurodegeneration. Transcript profiling data and the observed intralysosomal accumulation of cholesterol and gangliosides in CLN6-deficient fibroblasts suggest that disturbed cholesterol homeostasis is an important pathogenic cause. The cholesterol homeostasis block associated with a disruption of lipid/protein sorting mechanisms may lead to impairment of the function of the endosomal system.

2. Materials and methods

2.1. Cell lines

Cultured skin fibroblasts were obtained from 5 CLN6 patients belonging to 5 unrelated families (one American and four Portuguese). The American patient was homozygous for the mutation c.214G>T [3]. Three Portuguese patients were homozygous for c.460_462delATC leading to deletion of isoleucine 154. The other patient was a compound heterozygous carrying I154del mutation in one allele and [c.829_832delGTCTG; c.837delG] in the other resulting in a frameshift after tryptophan 276 [5]. These cases were previously reported as vLINCL patients [11]. In the Portuguese I154del homozygous patients the disease onset occurred around 4 years of age and skin biopsy was performed about 1 year and half later. Although the disease progression was similar until they became bedridden, the life expectancy was distinct. A similar disease progression was observed for the Portuguese I154del compound heterozygote. The ultrastructural study was performed later but a similar profile, a mix of curvilinear and fingerprint inclusions, was observed.

Fibroblasts were grown at 37 °C with 5% of CO₂ in Dulbecco's Medium, supplemented with antibiotics and 10% of fetal bovine serum. All culture reagents were purchased from GibcoBRL. All fibroblasts cell lines used were subjected to only two to three passages.

2.2. Affymetrix microarray data analysis

Global gene expression profiles were compared in human fibroblast cell lines from three normal adult individuals and five CLN6 patients. Total cellular RNA was isolated from 5×10^6 to 1×10^7 cells using Rneasy Mini Kit (Qiagen), according to manufacturer's instructions. Samples were analyzed using Affymetrix HuFL6800 GeneChip, which consists of probes for a total of 7129 human genes. After scanning probe arrays, data were stored, converted to .txt files, imported into Microsoft Excel, and used for data analysis and interpretation.

Genechip data were analyzed with the Affymetrix software, dChip, Microsoft Excel, Cluster, and S-plus (Seattle, WA) software. Raw data from Affymetrix CEL files were normalized and quantified using dChip [12]. Only genes with consistent hybridization indicators (AbsCall from Affymetrix software 5.0) from all replicates, and with greater than 2-fold changes (CLN6 deficient versus normal), were included. A further statistical test using modified *t*-test was performed using SAM software [13]. Expression levels were visualised by Cluster software with an established colour code, red for up-regulation, green for down-regulation. Classification of function of individual genes was based in part on information from LocusLink (<http://www.ncbi.nlm.nih.gov/LocusLink>).

2.3. Quantitation of mRNA by real time PCR

Total RNA was isolated from 5×10^6 to 1×10^7 cells using the Roche Applied Science Kit according to the manufacturer's manual. The RNA was reverse transcribed using the "First-strand cDNA synthesis kit" (Amersham Biosciences) following the manufacturer's protocol. Real-time PCR analysis was performed on an Applied Biosystems ABI PRISM 7000 Sequence Detection System. Primer and probe sequences (Table 1) were designed to specifically amplify cDNA using Primer Express software 2.0 or purchased as assays-on-demand (Applied Biosystems). PCR reactions were prepared in a final volume of 50 µl using 1× TaqMan Universal PCR Master Mix (Applied Biosystems), 300 nM of each primer, 250 nM of probe and 1 ng of RNA converted to cDNA. The conditions used for assays-on-demand were according to manufacturer's recommendations. Thermal cycling conditions comprised an initial AmpErase UNG incubation at 50 °C for 2 min, AmpliTaq Gold DNA Polymerase activation at 95 °C for 10 min, and 40 cycles of denaturation (95 °C for 15 s), annealing and extension (60 °C for 1 min). All PCR efficiencies were above 95%. Relative quantification of gene expression was performed using the standard curve method comprising four serial dilution points (ranging from 0.1 ng to 50 ng). For each sample, the RNA extraction procedure was repeated twice and each batch analyzed independently three times by calculating the average *C_t* values from duplicate PCR reactions. Glyceraldehyde 3-phosphate dehydrogenase (GAPDH, Applied Biosystems, #431098) gene expression was

Table 1
Primers and probes used in real time RT-PCR

Gene	GeneBank accession no.	Forward primer/Reverse primer/Probe	Exon boundary
AKR1C3/3 α -HSD	D17793	TGGAAAAGTAATATTTGACATAGTGGATCT GCCAATCCTGCATCCTTACAC TGTACCACCTGGGAGGCCATGGA	Exon 4/Exon 5
PP5/TFPI-2	D29992	CGATGCTTGCTGGAGGATAGA ACACTGGTTCGTCCACACTCACT AAAGTTCCCAAAGTTTGCCGGCTGC	Exon 2/Exon 3
GARP	Z24680	GCCATGAGACCCAGATCCT CTGGCAGAGACCTTCTTGTC CACAACACCAAGACAAAGTGCCCTGTAAGATG	Exon 2/Exon 3
BCHE	M16474	Hs00163746_m1 ^a	Exon 2/Exon 3
C1R	M14058	Hs00354278_m1 ^a	–
CSPG2	U16306	GCAAGATACCGAGACATGTGACTATG GACGGCATTCCCCTTCAG ACTTTGCCCATCGACGCACAT	–
CLU	NM_001831	Hs00156548_m1 ^a	Exon 3/Exon 4
HSP70-2/HSPA1B	M59830	ACCAAGCAGACGCAGATCTTC GCCCTCGTACCTGGATCA CCTACTCCGACAACCAACCCGGG	–
QPCT	X71125	Hs00202680_m1 ^a	Exon 2/Exon 3
CAV2	NM_001233	GATCCCCACCGGCTCAA ACCGGCTCTGCGATCACA TCGCATCTCAAGCTGGGCTTCGA	Exon 1/Exon 2
LOXL2	U89942	TGAAGAATGTCACCTGCGAGAA GATGTAGGCACCGCTCTCA ACGGACCTCGAGATTCCGAAAG	Exon 5/Exon 6
RRAS2	M31468	Hs00273367_m1 ^a	Exon 1/Exon 2
RAP1	X63465	Hs00221760_m1 ^a	Exon 12/Exon 13
RTVP-1	X91911	AACCAACAGCCAGTGATATGCTATAC GGCCCATGCTTTTGCAATT TGACTTGGGACCCAGCACTAGCCC	Exon 1/Exon 2
AIM1	U83115	GGAGACGATCATTTGCCGTTT CTTCTAGCAAATACTGATGACCGGTAA TCTATGAAAGTTCTAAGAGGCATTGGGTTGCAT	Exon 7/Exon 8

^a Primers and probes ordered to Applied Biosystems as assays-on-demand.

used for data normalization. All genes exhibited an interassay and intersample C_t variance ≤ 0.10 as assessed by variance using Excel computer software. The relative quantification of the mRNA was determined through the ratio of the normalized expressions of the CLN6 and control samples. *t*-test was used to assess differences in gene expression between patient and control cell lines. Two-sided *P* values of less than 0.05 were considered statistically significant. Data were expressed as a mean \pm SD.

2.4. Free cholesterol assay by filipin staining and fluorescence microscopy

Fibroblasts were stained with filipin and viewed by fluorescence microscopy according to Kruth et al. [14]. Briefly, cells were plated into chamber slides (Labteck slip, Nunc) in Dulbeccos MEM media (GibcoBRL) supplemented with 10% of fetal bovine serum, at 37 °C with 5% of CO₂ for 16 h. The media was replaced by MEM with 10% LPDS (Lipoprotein-deficient Serum, Sigma) and cells cultured for 3 days before human LDL was added (50 μ g/ml). The LDL fraction was prepared using blood from normal donors following the procedure described by Havel et al. [15]. After a 24-h incubation with LDL in 10% LPDS media, cells were washed with PBS (three times for 5 min), fixed with formaldehyde 3.7% (v/v) for 10 min at room temperature. After washing twice with PBS, 0.1 mg/ml of fresh Filipin (Sigma) was added to each slide and kept in the dark for 1 h. For colocalization study, after cell fixation they were permeabilized with 0.5% Triton X-100/PBS for 10 min at RT and blocked with PBS containing 1% bovine serum albumin (BSA) for 30 min. Cells were then incubated with mouse monoclonal (IgG1) Lamp 1 (H4A3) (Sigma) primary antibody previously diluted 1:100 in PBS for 12–16 h at 4 °C. The secondary antibody, chicken anti-mouse IgG-FITC (Sigma), diluted 1:100 in PBS was used

along with Filipin reagent. After washing in PBS, slides were mounted using VectaShield (Vector Laboratories) and visualised with a Nikon Eclipse E400 fluorescence microscope ($\lambda_{exc.}$ = 364 nm; $\lambda_{emi.}$ = 475 nm). Cells were imaged using a Nikon Coolpix 950 camera and processed with Adobe Photoshop CS V8.0 program.

2.5. Immunohistochemistry for human gangliosides

Cells were fixed with 3.7% formaldehyde in PBS pH 7.4 for 10 min at RT, rinsed twice with PBS, and permeabilized with 0.5% Triton X-100/PBS for 10 min at RT. After two washes, cells were blocked with PBS containing 1% bovine serum albumin (BSA) for 30 min. Cells were then incubated with monoclonal primary antibody anti-GM2 (IgM) [16], a kind gift from Dr. T. Tai from Metropolitan Institute of Medical Science in Japan, previously diluted 1:50 in PBS, for 12–16 h at 4 °C. After washing three times with PBS cells were incubated for 1 h with secondary antibody (anti-mouse (Fab')₂ IgM μ -chain specific, conjugated with fluoresceine) previously diluted 1:75 (Sigma). After washing with PBS, coverslips were mounted with VectorShield (Vector Laboratories), imaged with a Nikon Eclipse E400 fluorescence microscope ($\lambda_{exc.}$ = 494 nm; $\lambda_{emi.}$ = 518 nm) and charge-coupled device Nikon Coolpix 950 camera.

2.6. Assay for glycosaminoglycans in urine

Urine was collected over a period of 48 h keeping the sample refrigerated during collection. After collection aliquots were stored at –20 °C. Urinary creatinine was estimated using BioMérieux kit (BioMérieux, France) according to manufacturer's instructions. Quantification of total urinary glycosaminoglycans (GAGs) was performed by Alcian Blue complex formation method [17].



Fig. 1. Group of genes with altered expression (>2-fold) in CLN6-deficient human fibroblasts in comparison to normal. Colours represent relative levels of gene expression, with the brightest red indicating a higher level of gene expression, black indicating level of expression similar to normal and green depicting lower level of expression. Each horizontal line represents a gene; each column represents a cell line. Lanes 1 to 4 correspond to control cell lines; lanes 5 to 10 are CLN6 cell lines (5 and 6-homozygous for c.214G>T; 7, 9 and 10-homozygous for I154del; 8-compound heterozygous for I154del). (For interpretation of the references to colour in this figure legend, the reader is referred to the web version of this article.)

The GAG values were normalized to urinary creatinine and data expressed as mg GAG/mmol creatinine. Qualitative analysis of GAGs was determined by electrophoresis on cellulose acetate strips according to the procedure previously described [18], and expressed as percentage after densitometric scanning of Alcian Blue stained strips.

3. Results

3.1. Global gene expression changes in CLN6-deficient fibroblasts

Global gene expression patterns were generated from Affymetrix HuFL6800 Genechip microarrays using total RNA isolated from cultured skin fibroblasts from five CLN6 patients

and three normal controls. Using a 2-fold change in expression as the experimental cut-off that would imply significance, changes in gene expression were observed for 15 transcripts (Fig. 1), nine genes were up-regulated and six down-regulated compared to normal controls (Table 2). Those alterations were further confirmed by a second methodological approach, qRT-PCR (see below). Some other NCL-types were analyzed aside with CLN6 and control cell lines (data not shown). Distinct groups of genes with an altered expression profile were identified in other NCL-deficient fibroblasts, thus indicating that the expression profile here reported for CLN6 is specific of this variant. Of notice is the fact that higher variability in gene expression was observed for CLN6 cell lines than for other NCL-diseased fibroblasts tested using the same technical

Table 2
Gene expression profiling: expression changes greater than 2-fold in CLN6-human fibroblasts as compared to normal cell lines

Symbol	Description	Fold change	Expression level (mean±SD)	
			CLN6 ^a	Normal controls ^b
3α-HSD/AKR1C3	Aldo-keto reductase family I, member C3 (3-α-hydroxysteroid dehydrogenase, type II)	7.5	9109±4602	1216±559
TFPI-2	Tissue factor pathway inhibitor 2	6.2	6252±6001	1013±225
PP5	Placental protein 5	4.3	6532±4910	1507±973
GARP	Glycoprotein A repetitions predominant	3.7	7561±4557	2056±535
BCHE	Butyrylcholinesterase	3.1	269±85	86±15
C1R	Complement component 1, r subcomponent	2.9	14781±7746	5088±1266
CSPG2	Chondroitin sulphate proteoglycan 2 (versican)	2.8	9195±3049	3282±1458
TRPM2/CLU	Testosterone-repressed message 2 (clusterin, complement lysis inhibitor, SP-40, sulfated glycoprotein 2, apolipoprotein J)	2.8	14398±5097	5229±1228
HSPA1B7 HSP70-2	Human HMC class III heat shock HSP70-2 gene (HLA), 70 kDa protein 1B	2.5	3033±2389	1217±155
QPCT	Glutaminy-peptide cyclotransferase (glutaminy cyclase)	2.1	2049±405	991±405
CAV2	Caveolin 2	−2.0	3086±1381	6106±1388
LOXL2	Lysyl oxidase-like 2	−2.0	4704±2753	9512±1077
RRAS2	Ras-like protein TC21	−2.0	2999±1003	6088±1947
RAP1	GTP-GDP dissociation stimulator 1	−2.2	1055±347	2285±1032
RTVP1	Glioma pathogenesis-related protein/RTVP-1 protein	−2.3	3088±1102	6951±1928
AIM1	Absent in melanoma 1/Human non-lens beta gamma-crystallin like complex	−2.9	964±300	2759±905

TFPI2 and PP5 refer to the same gene. Fold change is calculated as ratio between the CLN6 and normal control cell lines. Expression levels were taken as Affymetrix Average Difference values (arbitrary units).

^a Mean expression values from CLN6 patients, *n*=5.

^b Mean expression values from normal controls, *n*=3.

approach. Perhaps this could reflect biological variability associated with the CLN6 deficiency. If this variability has physiological meaning at either protein or phenotypic level is presently unknown.

3.2. Validation of gene expression profile by real-time RT-PCR (qRT-PCR)

RNA was isolated from CLN6-deficient cell patients and normal human fibroblasts and used to examine the expression of the 16 genes by qRT-PCR (TaqMan chemistry) in order to validate cDNA microarray data. For normalization purposes, the housekeeping gene GAPDH was used. This gene has been widely used as a constitutively expressed control gene in RT-PCR studies [19]. Moreover, microarray data showed that its expression remained unchanged in CLN6-deficient cells when compared with control cells (1.04-fold). Under the qRT-PCR experimental conditions, BCHE gene expression level was undetectable. This result was not surprising since genechip profiling revealed a significantly lower expression level for BCHE as compared with all the other genes (Table 2). TFPI2 and PP5 refer to the same gene and are, therefore, treated as one. TFPI2 is the designation used throughout the text.

Data obtained for the remaining 14 transcripts is presented in Table 3. From the set of fourteen genes, 12 (86%) had a statistically significant fold change in qRT-PCR ($P < 0.05$). For the remaining two, HSP70-2 and RAP21, with a mean fold change of 1.2 and 1.1 respectively; the expression was considered unchanged between CLN6 and control cells. The qRT-PCR confirmed expression changes observed in genechip profiling for 7 up-regulated genes (about 60% of total). The remaining 5 genes down-regulated in microarray were found up-regulated by qRT-PCR. This apparent discrepancy can be explained by the low differential expression (2.3-fold or less)

observed in microarray analysis for most of down-regulated genes. Furthermore, microarray data can be implicated by cross-hybridization from other genes [20], even though the observations are statistically consistent. On the other hand, real time allowed the detection of 1.5-fold change, or even less, implying that changes in expression of genes can be detected with higher reproducibility and sensitivity by qRT-PCR than genechip profiling. Thus, using microarray to rapidly screen the transcriptome disease and then validating the results by gene-specific qRT-PCR, may lead to reliable disease biomarkers.

3.3. Functional categorization of gene products

The 12 up-regulated genes can be grouped into 4 functional categories: extracellular matrix (ECM) remodelling, cell signalling, apoptosis and immuno/inflammatory response. Since many of these genes have more than one function, they could be assigned to more than one functional class. About 60% of the overexpressed genes in CLN6-deficient cells are related to cell surface, cell adhesion, cell proliferation and cytoskeleton. This category reflects the overlap that may occur between the functions of proteins located at the cell surface. It includes CSPG2, LOXL2, TFPI2, GARP [21,22], RTVP1, TC21, AIM1 and CLU. The most pronounced expression changes were observed for versican (CSPG2) [23–25] and the tissue factor pathway inhibitor 2 (TFPI-2), a serine protease inhibitor reported at high levels in extracellular matrix [26,27], supporting a role for CLN6 in ECM remodelling.

The group of genes related to apoptosis include CSPG2, LOXL2 [28], RTVP1, AIM1 and CLU. Up-regulation of genes encoding molecular chaperones, namely clusterin and small heat shock proteins AIM1 is not surprising since the storage material in CLN6-deficient cells is mainly of a proteinaceous nature. The overexpression of these genes may protect CLN6 cells against apoptotic cell death induced by heat shock, oxidative stress and neurodegeneration, as reported for other neurodegenerative conditions [29–32]. Component C1R [33] and clusterin [34,35] (also implicated in inhibition of complement attack) have also been associated with the immuno/inflammatory response. Overexpression of TFPI-2 in CLN6-deficient cell lines is observed. An anti-inflammatory function is attributed to its inhibitory role of matrix metalloproteinases involved in ECM architecture remodelling [36]. The advancement of both proinflammatory and anti-inflammatory mechanisms probably suggests the secondary nature of inflammation in the neurodegenerative process.

Gene expression profiling also suggests the involvement of diverse signalling molecules in the pathogenesis of CLN6. The gene products included in this category dictate alterations in neurotransmission (QPCT and 3 α -HSD), steroidogenic hormones (3 α -HSD and CLU) and intracellular signalling cascades (CAV2 and TC21) [37].

3.4. Cholesterol, gangliosides and GAGs imbalance in CLN6-deficient fibroblasts

The altered expression profile of a set of genes comprising 3 α -HSD, CSPG2, LOXL2, QPCT, CLU and CAV2 implies

Table 3
Relative quantitation of transcripts by real time RT-PCR

Gene	qRT-PCR				Genechip
	Expression level (mean±SD)		Mean fold change	<i>P</i>	Mean fold change
	CLN6 ^a	Normal controls ^b			
3α-HSD	5.15±3.37	1.00±0.06	5.2	<0.05	7.5
TFPI2/PP5	20.0±15.9	1.00±0.13	20	<0.05	4.3
GARP	4.98±2.31	1.00±0.11	5.0	<0.05	3.7
C1R	3.10±0.55	1.00±0.14	3.1	<0.005	2.9
CSPG2	48.1±23.3	1.00±0.09	48	<0.05	2.8
TRPM2	1.47±0.34	1.00±0.19	1.5	<0.05	2.8
HSP70-2	1.22±0.43	1.00±0.11	1.2		2.5
QPCT	2.59±0.28	1.00±0.25	2.5	<0.005	2.1
CAV2	1.59±0.24	1.00±0.11	1.6	<0.005	−2.0
LOXL2	9.98±4.11	1.00±0.08	10.0	<0.05	−2.0
TC21	3.92±1.19	1.00±0.11	3.9	<0.005	−2.0
RAP1	1.14±0.20	1.00±0.08	1.1		−2.2
RTVP1	5.03±3.00	1.00±0.04	5.0	<0.05	−2.3
AIM1	2.22±0.67	1.00±0.07	2.2	<0.05	−2.9

Fold change is calculated as ratio between the CLN6 and normal control cell lines.

^a Mean expression values from CLN6 patients, $n = 3$.

^b Mean expression values from normal controls, $n = 2$.

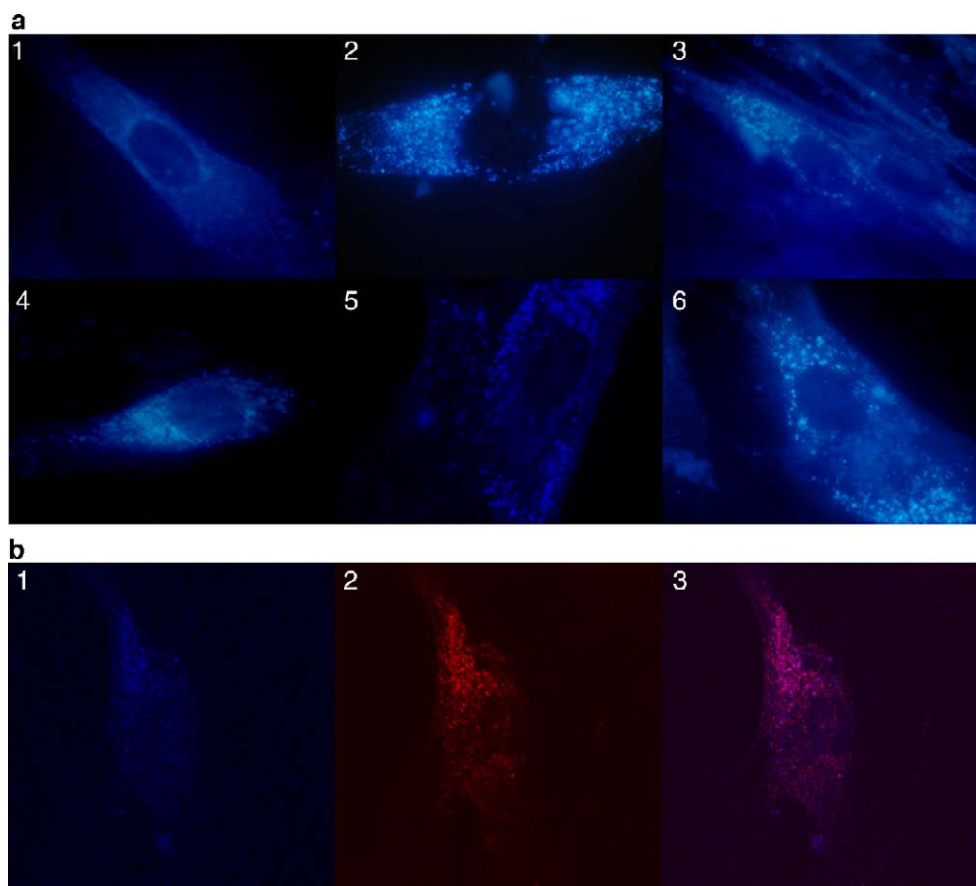


Fig. 2. (a) Evaluation of free cholesterol accumulation by Filipin Staining. Cells from individuals with: 1-no pathology; 2-Niemann–Pick type C; 3-GM1-Gangliosidosis; 4-GM2-Gangliosidosis (B1 variant); 5 and 6-CLN6 variant (homozygous for I154del, lane 10 of Fig. 1, and compound heterozygous for I154del, lane 8 of Fig. 1, respectively). (b) Co-localization of Filipin Staining with the lysosomal marker, Lamp 1. Cells from a CLN6 cell line (lane 10 of Fig. 1): 1-with Filipin staining; 2-marked with Lamp 1; 3-co-localization of Filipin staining with Lamp 1.

alterations in cholesterol as precursor for steroid hormones, structure of lipid rafts and cofactor for signalling [38–44,30]. The observed expression changes would reflect physiological compensatory mechanisms aiming to restore cholesterol homeostasis in CLN6 disease. To address this hypothesis filipin staining of CLN6-deficient human fibroblasts was performed to detect free cholesterol. Cells from patients with Niemann–Pick type C (NPC), gangliosidosis GM1 and GM2 (B1 variant) were used as positive controls (Fig. 2a). Similarly to NPC and gangliosidoses, CLN6-deficient cells cultured in the presence of LDL showed filipin staining in perinuclear granules reflective of lysosomal cholesterol accumulation. In normal control fibroblasts relatively little cytoplasmatic fluorescence was observed. The lysosomal distribution of the accumulated free

cholesterol in CLN6-deficient human fibroblasts was confirmed by colocalization assay using Lamp 1 as lysosomal marker (Fig. 2b). Secondary glycosphingolipid accumulation has been documented in human fibroblasts [45] and mouse models of several LSDs [46]. This storage is accompanied by sequestration of free cholesterol in a manner similar to that observed in primary gangliosidoses [47]. We investigated the accumulation of ganglioside GM2 in CLN6-deficient fibroblasts by immunofluorescence microscopy. Discrete punctate fluorescent structures outlining the region of the nucleus were visualised and appeared identical to those observed in NPC and GM2-gangliosidoses (B1 variant) (Fig. 3). Secondary accumulation of gangliosides related to a cholesterol disturbed homeostasis might explain their intralysosomal trapping in CLN6 deficient

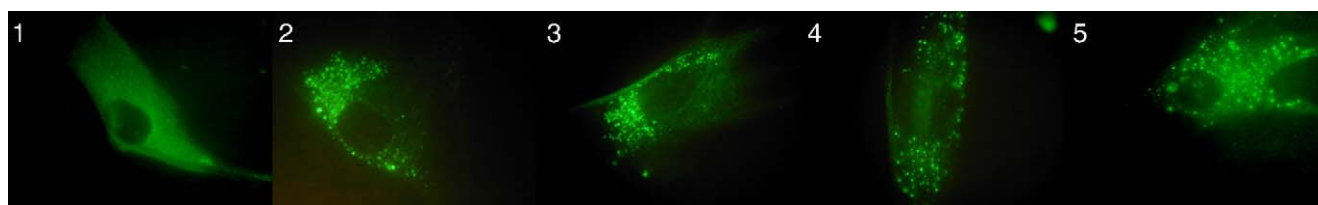


Fig. 3. GM2 ganglioside accumulation in LSD skin fibroblasts. Cell lines from individuals with: 1-no pathology; 2-GM2-Gangliosidosis (B1 variant); 3-Niemann–Pick type C; 4 and 5-CLN6 variant (homozygous for I154del, lane 10 of Fig. 1, and compound heterozygous for I154del, lane 8 of Fig. 1, respectively).

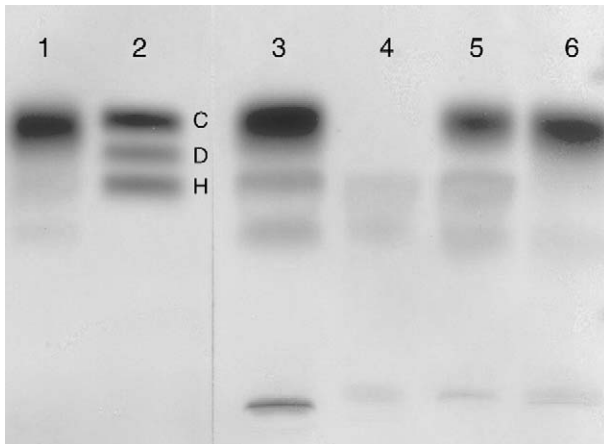


Fig. 4. Glycosaminoglycan profile in urine from a CLN6 homozygous patient for I154del. The level of GAGs was determined by Alcian Blue method. GAG composition was assessed by monodimensional cellulose acetate gel electrophoresis. Urine samples: lane 1-control individual; lane 2-C, D and H refer to the chondroitin sulphate, dermatan sulphate and heparin sulphate standards, respectively; lane 3-CLN6 patient; lane 4-CLN6 patient after chondroitinase ABC digestion; lane 5-CLN6 patient after chondroitinase B (dermatan sulphate) digestion; lane 6-CLN6 patient after heparitinase III digestion.

human fibroblasts. A fainter staining was observed in one I154del homozygous patient but it is presently unclear if that variability has any physiological meaning.

The two most over-expressed gene products (CSPG2 and TFPI2) are related to abnormal turnover of proteoglycans. Urinary GAGs were analyzed as a measure of lysosomal storage in the kidney tubules, and, by association, as a measure of overall storage in other tissues. Two samples of urine were collected from a CLN6-deficient patient homozygous for the mutation I154del, at 15 and 17 years of age. The excreted GAG mean level was higher when compared to normal age-matched controls (8.0 mg/mmol creatinine; normal: 2.0–6.5 mg/mmol creatinine). GAG profile was distinct in this patient as compared with control urines (Fig. 4). In control urines only one band (lane 1) co-migrating with chondroitin sulphate was observed. In contrast, in the CLN6-deficient patient urine three bands (lane 3) were clearly observed. One large band co-migrating with chondroitin sulphate and dermatan sulphate standards disappeared after digestion with chondroitinase ABC (lane 4). Digestion with chondroitinase B (lane 5) resulted in a band co-migrating with chondroitin sulphate. This profile suggests a higher heterogeneity of the chondroitin sulphates in CLN6 urines in comparison with control samples. The other band co-migrating with heparin sulphate standard was sensitive to heparitinase digestion (lane 6). By densitometry, heparin sulphate was estimated to correspond to about 25% of total GAGs and was about 4-fold higher than controls.

4. Discussion

The variant late infantile form of NCL is a pan-ethnic disease caused by mutations in the CLN6 gene. Typical inclusions are seen in neuronal and other cell types. We hypothesized that the gene expression profile of CLN6-deficient fibroblasts can provide valuable clues into the molecular pathophysiological

mechanisms operating in this disease. We analyzed global gene expression by cDNA genechip profiling and used real time RT-PCR to validate the microarray data. Fifteen genes were found differentially expressed by genechip profile, and twelve presented statistically significant changes by qRT-PCR. The set of genes found up-regulated in CLN6-deficient fibroblasts suggests a modulation of architecture of cell surface and signal transduction pathways, apoptosis and immune/inflammatory response in CLN6 variant.

The most remarkable over-expressed gene product was versican (CSPG2), a cell surface proteoglycan whose glycosaminoglycan segment is a linear sulfated polysaccharide of chondroitin-6-sulfate. CSPGs are major components of brain extracellular matrix interacting with other matrix proteins, cell surface receptors and transporters. Thus, the overexpression of versican suggests alterations in cell–cell communication and intracellular organization through either cytoskeleton rearrangement or modulation of trafficking pathways. The altered expression of a set of genes, including TC21 and CAV2, supports the importance of lipid raft signalling cascades in CLN6-deficiency pathogenesis. For TC21, a member of the Ras superfamily of small GTP-binding proteins, effector pathways include Ral, phosphatidylinositol 3' kinase and Ras/Raf/MAP kinase pathways [48]. Interestingly, the Ras/Raf/MAPK signalling cascade regulates the expression of the ECM protease inhibitor TFPI2 [49,50] found to be overexpressed in CLN6-deficient cells. Caveolin 2 is known to be present in specialized lipid domains, caveolae, and acting as small signalling compartments. In addition to concentrating signal transducers, caveolin binding may functionally regulate the activation state of caveolae-associated signalling molecules [51].

The altered expression of caveolin 2 and other gene products related to cholesterol (3 α -HSD, CSPGs, LOXL2, QPCT and clusterin) point to a cholesterol homeostasis break as a consequence of CLN6 deficiency.

No cholesterol accumulation was observed by HPTLC (unpublished results) corroborating data of previous studies in CLN6-deficient animals using the same methodology [52]. Fluorescence microscopy of CLN6-deficient fibroblasts however showed intracellular accumulation of cholesterol in lysosomes (Fig. 2b). In addition to cholesterol, these cells were also found to accumulate gangliosides. Given that GSLs and cholesterol are constituents of caveolae and lipid rafts critical for signal transduction events, in neurons and other cells, their co-sequestration in lysosomes predicts defects in the composition, trafficking, and/or recycling of raft components that may affect endocytic function, [47,53], including lysosome biogenesis and autophagy. These alterations would lead to the accumulation of a broad spectrum of substrates as observed in NCL disease. Interestingly, the involvement of lipid rafts and vesicular trafficking in CLNp cell biology and pathophysiology is not without precedent. Several lines of evidence suggest that CLN3p follows the constitutive cell route, from ER to Golgi to plasma membrane via early endosomes. Faulty trafficking leads to accumulation of CLN3p and galactosylceramide in lysosomes [54]. In these routes, whether exocytic, endocytic or both, CLN3p has been localized to lipid rafts [55].

In addition to lipid accumulation, an abnormal pattern of GAGs was observed in the urine of an I154del homozygous patient. As far as we know skeletal abnormalities have never been reported for CLN6 patients. Nevertheless, GAGs, such as heparan sulfate and dermatan sulfate (chondroitin sulfate B), were recently reported to stimulate the activation of pro-TPP1 and to inhibit the *in vitro* and *in vivo* activity of mature enzyme in a dose dependent manner [56]. Interestingly, in CLN2-deficient cells we have also observed an overexpression of versican by qRT-PCR (data not shown). Like TPP1, a pH-dependent inhibition of enzyme activity by GAGs has been documented for other lysosomal enzymes [57,58], and alterations in intralysosomal pH have been reported in fibroblasts from patients with different forms of NCL, including CLN6 [59]. It may be that a pH-dependent inhibition of GSL-degradative enzymes by GAGs contributes to secondary storage of glycosphingolipids in CLN6-deficient cells.

Many of the transcripts up-regulated in CLN6 deficient human fibroblasts are known to be expressed in the brain [23,60–65,40]. Interestingly, 3 α -HSD is known to regulate the occupancy of the γ -aminobutyric acid (GABA) receptor by converting 5 α -dihydroprogesterone into 3 α -hydroxy-5 α -pregnan-20-one (allopregnanolone), a potent positive allosteric effector of the GABA receptor chloride ion channel [38]. Recently, a substantial reduction in the synthesis of allopregnanolone has been reported in a mouse model for Niemann–Pick type C, and administration of allopregnanolone delayed disease progression [66,67]. Allopregnanolone is an anticonvulsant neurosteroid [68], thus, the up-regulation of 3 α -HSD, as observed in CLN6 deficient fibroblasts, may suggest a compensatory mechanism for modulation of seizure susceptibility in patients. Given the role of cholesterol in synaptic formation and function, plasticity and neurodegeneration [69,70], disruption of cholesterol homeostasis may contribute to pathogenesis of neurodegenerative CLN6-deficiency.

In conclusion, the data reported here suggest that a disruption of cholesterol homeostasis in CLN6 disease, in addition to changes in extracellular matrix architecture remodelling, signalling cascades and intracellular vesicular trafficking may be important pathogenic factors. A balance between apoptotic and anti-apoptotic mechanisms, as well as proinflammatory and anti-inflammatory processes, may also contribute to disease progression and severity. For the time being it is impossible to know the precise sequence of the cellular events that eventually will lead to development of the disease, i.e., which have a causal role and which are more secondary as a reflection of a primary event. It is reasonable to assume that once the cascade of events is initiated each cellular response will have a retrograde effect on the other cellular responses perhaps exacerbating their effect on disease progression.

Acknowledgements

The study would not have been possible without the generous cooperation of the patients and their families. The authors thank I. B.M.C for providing financial support for genechip analysis. This work was supported by FCT, POCTI and FEDER (grant 33172/MGI/2000; doctoral fellowship SFRH/BD/1466/2000 to T.C.A.F.;

research fellowship to M.M.), and l'Association Vaincre les Maladies Lysosomales (doctoral fellowship to B.C.J.P.).

References

- [1] S.E. Mole, R.E. Williams, H.H. Goebel, Correlations between genotype, ultrastructural morphology and clinical phenotype in the neuronal ceroid lipofuscinoses, *Neurogenetics* 6 (2005) 107–126.
- [2] J. Ezaki, K. Eiki, The intracellular location and function of proteins of neuronal ceroid lipofuscinoses, *Brain Pathol.* 14 (2004) 77–85.
- [3] H. Gao, R.M. Boustany, J.A. Espinola, S.L. Cotman, L. Srinidhi, K.A. Antonellis, T. Gillis, X. Qin, S. Liu, L.R. Donahue, R.T. Bronson, J.R. Faust, D. Stout, J.L. Haines, T.J. Lerner, M.E. MacDonald, Mutations in a novel CLN6-encoded transmembrane protein cause variant neuronal ceroid lipofuscinosis in man and mouse, *Am. J. Hum. Genet.* 70 (2) (2002) 324–335.
- [4] R.B. Wheeler, J.D. Sharp, R.A. Schultz, J.M. Joslin, R.E. Williams, S.E. Mole, The gene mutated in variant late-infantile neuronal ceroid lipofuscinosis (CLN6) and in *nclf* mutant mice encodes a novel predicted transmembrane protein, *Am. J. Hum. Genet.* 70 (2) (2002) 537–542.
- [5] C.A. Teixeira, J. Espinola, L. Huo, J. Kohlschutter, D.A. Persaud Sawin, B. Minassian, C.J. Bessa, A. Guimaraes, D.A. Stephan, M.C. Sa Miranda, M.E. MacDonald, M.G. Ribeiro, R.M. Boustany, Novel mutations in the CLN6 gene causing a variant late infantile neuronal ceroid lipofuscinosis, *Human Mutat.* 21 (5) (2003) 502–508.
- [6] J.D. Sharp, R.B. Wheeler, K.A. Parker, R.M. Gardiner, R.E. Williams, S.E. Mole, Spectrum of CLN6 mutations in variant late infantile neuronal ceroid lipofuscinosis, *Human Mutat.* 22 (1) (2003) 35–42.
- [7] C. Heine, B. Koch, S. Storch, A. Kohlschutter, D.N. Palmer, T. Bräulke, Defective endoplasmic reticulum-resident membrane protein CLN6 affects lysosomal degradation of endocytosed arylsulfatase A, *J. Biol. Chem.* 279 (21) (2004) 22347–22352.
- [8] S.E. Mole, G. Michaux, S. Codlin, R.B. Wheeler, J.D. Sharp, D.F. Cutler, CLN6, which is associated with a lysosomal storage disease, is an endoplasmic reticulum protein, *Exp. Cell Res.* 298 (2004) 399–406.
- [9] L. Lonka, A. Kytälä, S. Ranta, A. Jalanko, A.E. Lehesjoki, The neuronal ceroid lipofuscinosis CLN8 membrane protein is a resident of the endoplasmic reticulum, *Hum. Mol. Genet.* 9 (11) (2000) 1691–1697.
- [10] E. Winter, C.P. Ponting, TRAM, LAG1 and CLN8: members of a novel family of lipid-sensing domains? *Trends Biochem. Sci.* 27 (8) (2002) 381–383.
- [11] C. Teixeira, A. Guimaraes, C. Bessa, M.J. Ferreira, L. Lopes, E. Pinto, R. Pinto, R.M. Boustany, M.C. Sa Miranda, M.G. Ribeiro, Clinicopathological and molecular characterization of neuronal ceroid lipofuscinosis in the Portuguese population, *J. Neurol.* 250 (6) (2003) 661–667.
- [12] C. Li, W.H. Wong, Model-based analysis of oligonucleotide arrays: expression index computation and outlier detection, *Proc. Natl. Acad. Sci. U. S. A.* 98 (1) (2001) 31–36.
- [13] V.G. Tusher, R. Tibshirani, G. Chu, Significance analysis of microarrays applied to the ionizing radiation response, *Proc. Natl. Acad. Sci. U. S. A.* 98 (9) (2001) 5116–5121.
- [14] H.S. Kruth, M.E. Comly, J.D. Butler, M.T. Vanier, J.K. Fink, D.A. Wenger, S. Patel, P.G. Pentchev, Type C Niemann–Pick disease. Abnormal metabolism of low density lipoprotein in homozygous and heterozygous fibroblasts, *J. Biol. Chem.* 261 (1986) 16769–16774.
- [15] R.J. Havel, H.A. Eder, J.H. Bragdon, *J. Clin. Invest.* 34 (1955) 1345–1353.
- [16] M. Kotani, H. Ozawa, I. Kawashima, S. Ando, T. Tai, Generation of one set of monoclonal antibodies specific for a-pathway ganglio-series gangliosides, *Biochim. Biophys. Acta* 1117 (1) (1992) 97–103.
- [17] P. Whiteman, H. Henderson, A method for the determination of amniotic-fluid glycosaminoglycans and its application to the prenatal diagnosis of Hurler and Sanfilippo diseases, *Clin. Chim. Acta* 79 (1977) 99–105.
- [18] J.J. Hopwood, J.R. Harrison, High resolution electrophoresis of urinary glycosaminoglycans: an improved screening test for the MPS, *Anal. Biochem.* 119 (1982) 120–127.
- [19] J. Vandesompele, K. De Preter, F. Pattyn, B. Poppe, N. Van Roy, A. De Paepe, F. Speleman, Accurate normalization of real-time quantitative

- RT-PCR data by geometric averaging of multiple internal control genes, *Genome Biol.* 3 (7) (2002) 1–12.
- [20] C.C. Chou, C.H. Chen, T.T. Lee, K. Peck, Optimization of probe length and the number of probes per gene for optimal microarray analysis of gene expression, *Nucleic Acids Res.* 32 (12) (2004) e99.
 - [21] R. Roubin, S. Pizette, V. Ollendorff, J. Planche, D. Birnbaum, O. Delapeyriere, Structure and developmental expression of mouse Garp, a gene encoding a new leucine-rich repeat-containing protein, *Int. J. Dev. Biol.* 40 (3) (1996 Jun) 545–555.
 - [22] R. Legouis, F. Jaulin-Bastard, S. Schott, C. Navarro, J.P. Borg, M. Labouesse, Basolateral targeting by leucine-rich repeat domains in epithelial cells, *EMBO Rep.* 4 (11) (2003 Nov) 1096–1102.
 - [23] M. Grumet, D.R. Friedlander, T. Sakurai, Functions of brain chondroitin sulfate proteoglycans during developments: interactions with adhesion molecules, *Perspect. Dev. Neurobiol.* 3 (4) (1996) 319–330.
 - [24] R.A. Asher, D.A. Morgenstern, M.C. Shearer, K.H. Adcock, P. Pesheva, J.W. Fawcett, Versican is upregulated in CNS injury and is a product of oligodendrocyte lineage cells, *J. Neurosci.* 22 (6) (2002 Mar 15) 2225–2236.
 - [25] F. Matsui, A. Oohira, Proteoglycans and injury of the central nervous system, *Congenit. Anom. (Kyoto)* 44 (4) (2004 Dec) 181–188.
 - [26] M. Iino, D.C. Foster, W. Kisiel, Quantification and characterization of human endothelial cell-derived tissue factor pathway inhibitor-2, *Arterioscler. Thromb. Vasc. Biol.* 18 (1) (1998) 40–46.
 - [27] C.N. Rao, B. Cook, Y. Liu, K. Chilukuri, M.S. Stack, D.C. Foster, W. Kisiel, D.T. Woodley, HT-1080 fibrosarcoma cell matrix degradation and invasion are inhibited by the matrix-associated serine protease inhibitor TFPI-2/33 kDa MSPI, *Int. J. Cancer* 76 (5) (1998 May 29) 749–756.
 - [28] K. Csiszar, Lysyl oxidases: a novel multifunctional amine oxidase family, *Prog. Nucleic Acid Res. Mol. Biol.* 70 (2001) 1–32.
 - [29] S.E. Jones, J.M. Meerabux, D.A. Yeats, M.J. Neal, Analysis of differentially expressed genes in retinitis pigmentosa retinas, Altered expression of clusterin mRNA, *FEBS Lett.* 300 (3) (1992) 279–282.
 - [30] M. Calero, A. Rostagno, E. Matsubara, B. Zlokovic, B. Frangione, J. Ghiso, Apolipoprotein J (clusterin) and Alzheimer's disease, *Microsc. Res. Tech.* 50 (4) (2000) 305–315.
 - [31] A.I. Brooks, S. Chattopadhyay, H.M. Mitchison, R.L. Nussbaum, D.A. Pearce, Functional categorization of gene expression changes in the cerebellum of a Cln3-knockout mouse model for Batten disease, *Mol. Genet. Metab.* 78 (1) (2003) 17–30.
 - [32] J. Graw, The crystallins: genes, proteins and diseases, *Biol. Chem.* 378 (11) (1997) 1331–1348.
 - [33] K. Yasojima, C. Schwab, E.G. McGeer, P.L. McGeer, Up-regulated production and activation of the complement system in Alzheimer's disease brain, *Am. J. Pathol.* 154 (3) (1999 Mar) 927–936.
 - [34] P. Wong, T. Ulyanova, D.T. Organisciak, S. Bennett, J. Lakins, J.M. Arnold, R.K. Kutty, M. Tenniswood, T. vanVeen, R.M. Darrow, G. Chader, Expression of multiple forms of clusterin during light-induced retinal degeneration, *Curr. Eye Res.* 23 (3) (2001 Sep) 157–165.
 - [35] S. Poon, T.M. Treweek, M.R. Wilson, S.B. Easterbrook-Smith, J.A. Carver, Clusterin is an extracellular chaperone that specifically interacts with slowly aggregating proteins on their off-folding pathway, *FEBS Lett.* 513 (2–3) (2002 Feb 27) 259–266.
 - [36] M.P. Herman, G.K. Sukhova, W. Kisiel, D. Foster, M.R. Kehry, P. Libby, U. Schönbeck, Tissue factor pathway inhibitor-2 is a novel inhibitor of matrix metalloproteinases with implications for atherosclerosis, *J. Clin. Invest.* 107 (9) (2001) 1117–1126.
 - [37] W.M. Krajewska, I. Maslowska, Caveolins: structure and function in signal transduction, *Cell. Mol. Biol. Lett.* 9 (2) (2004) 195–220.
 - [38] T.M. Penning, M.E. Burczynski, J.M. Jez, C.F. Hung, H.K. Lin, H. Ma, M. Moore, N. Palackal, K. Ratnam, Human 3 α -hydroxysteroid dehydrogenase isoforms (AKR1C1–AKR1C4) of the aldo-keto reductase superfamily: functional plasticity and tissue distribution reveals roles in the inactivation and formation of male and female sex hormones, *Biochem. J.* 351 (Pt 1) (2000) 67–77.
 - [39] S. Swarnakar, J. Beers, D.K. Strickland, S. Azhar, D.L. Williams, The apolipoprotein E-dependent low density lipoprotein cholesteryl ester selective uptake pathway in murine adrenocortical cells involves chondroitin sulfate proteoglycans and an alpha 2-macroglobulin receptor, *J. Biol. Chem.* 276 (24) (2001) 21121–21128.
 - [40] C. Jourdan-Le Saux, H. Tronecker, L. Bogic, G.D. Bryant-Greenwood, C.D. Boyd, K. Csiszar, The LOXL2 gene encodes a new lysyl oxidase-like protein and is expressed at high levels in reproductive tissues, *J. Biol. Chem.* 274 (18) (1999) 12939–12944.
 - [41] W.H. Fischer, J. Spiess, Identification of a mammalian glutaminyl cyclase converting glutaminyl into pyroglutaminyl peptides, *Proc. Natl. Acad. Sci. U. S. A.* 84 (11) (1987) 3628–3632.
 - [42] S. Roy, R. Luetterforst, A. Harding, A. Apolloni, M. Etheridge, E. Stang, B. Rolls, J.F. Hancock, R.G. Parton, Dominant-negative caveolin inhibits H-Ras function by disrupting cholesterol-rich plasma membrane domains, *Nat. Cell Biol.* 1 (2) (1999 Jun) 98–105.
 - [43] M. Stahlhut, K. Sandvig, B. van Deurs, Caveolae: uniform structures with multiple functions in signaling, cell growth, and cancer, *Exp. Cell Res.* 261 (1) (2000 Nov 25) 111–118.
 - [44] P.W. Sternberg, S.L. Schmid, Caveolin, cholesterol and Ras signalling, *Nat. Cell Biol.* 1 (2) (1999 Jun) E35–E37.
 - [45] R.E. Pagano, V. Puri, M. Dominguez, D.L. Marks, Membrane traffic in sphingolipid storage diseases, *Traffic* 1 (11) (2000) 807–815.
 - [46] R. McGlynn, K. Dobrenis, S.U. Walkley, Differential subcellular localization of cholesterol, gangliosides, and glycosaminoglycans in murine models of mucopolysaccharide storage disorders, *J. Comp. Neurol.* 480 (4) (2004) 415–426.
 - [47] V. Puri, R. Watanabe, M. Dominguez, X. Sun, C.L. Wheatley, D.L. Marks, R.E. Pagano, Cholesterol modulates membrane traffic along the endocytic pathway in sphingolipid-storage diseases, *Nat. Cell Biol.* 1 (6) (1999) 386–388.
 - [48] M. Rosario, H.F. Paterson, C.J. Marshall, Activation of the Ral and phosphatidylinositol 3' kinase signalling pathways by the ras-related protein TC21, *Mol. Cell. Biol.* 21 (11) (2001) 3750–3762.
 - [49] R. Khosravi-Far, S. Campbell, K.L. Rossman, C.J. Der, Increasing complexity of Ras signal transduction: involvement of Rho family proteins, *Adv. Cancer Res.* 72 (1998) 57–107.
 - [50] C. Kast, M. Wang, M. Whiteway, The ERK/MAPK pathway regulates the activity of the human tissue factor pathway inhibitor-2 promoter, *J. Biol. Chem.* 278 (2003) 6787–6794.
 - [51] T. Okamoto, A. Schlegel, P.E. Scherer, M.P. Lisanti, Caveolins, a family of scaffolding proteins for organizing “preassembled signalling complexes” at the plasma membrane, *J. Biol. Chem.* 273 (10) (1998) 5419–5422.
 - [52] D.N. Palmer, D.R. Husband, P.J. Winter, J.W. Blunt, R.D. Jolly, Ceroid lipofuscinosis in sheep: I. Bis(monoacylglycerol)phosphate, dolichol, ubiquinone, phospholipids, fatty acids, and fluorescence in liver lipopigment lipids, *J. Biol. Chem.* 261 (4) (1986) 1766–1772.
 - [53] A. Choudhury, M. Dominguez, V. Puri, D.K. Sharma, K. Narita, C.L. Wheatley, D.L. Marks, R.E. Pagano, Rab proteins mediate Golgi transport of caveola-internalized glycosphingolipids and correct lipid trafficking in Niemann–Pick C cells, *J. Clin. Invest.* 109 (12) (2002) 1541–1550.
 - [54] D.A. Persaud-Sawin, J.O. McNamara II, S. Rylova, A. Vandongen, R.M. Boustany, A galactosylceramide binding domain is involved in trafficking of CLN3 from Golgi to rafts via recycling endosomes, *Pediatr. Res.* 56 (3) (2004) 449–463.
 - [55] D. Rakheja, S.B. Narayan, J.V. Pastor, M.J. Bennett, CLN3P, the Batten disease protein, localizes to membrane lipid rafts (detergent-resistant membranes), *Biochem. Biophys. Res. Commun.* 317 (4) (2004) 988–991.
 - [56] A.A. Golabek, M. Walus, K.E. Wisniewski, E. Kida, Glycosaminoglycans modulate activation, activity, and stability of tripeptidyl-peptidase I in vitro and in vivo, *J. Biol. Chem.* 280 (9) (2005) 7550–7561.
 - [57] P.C. Almeida, I.L. Nantes, J.R. Chagas, C.C. Rizzi, A. Faljoni-Alario, E. Carmona, L. Juliano, H.B. Nader, I.L. Tersariol, Cathepsin B activity regulation. Heparin-like glycosaminoglycans protect human cathepsin B from alkaline pH-induced inactivation, *J. Biol. Chem.* 276 (2) (2001) 944–951.
 - [58] A.R. Rushton, G. Dawson, The effect of glycosaminoglycans on the in vitro activity of human skin fibroblast glycosphingolipid beta-galactosidases and neuraminidases, *Clin. Chim. Acta* 80 (1) (1977) 133–139.
 - [59] J.M. Holopainen, J. Saarikoski, P.K. Kinnunen, I. Jarvela, Elevated lysosomal pH in neuronal ceroid lipofuscinoses (NCLs), *Eur. J. Biochem.* 268 (22) (2001) 5851–5856.

- [60] S.D. Konduri, K.S. Srivenugopal, N. Yanamandra, D.H. Dinh, W.C. Olivero, M. Gujrati, D.C. Foster, W. Kisiel, F. Ali-Osman, S. Kondraganti, S.S. Lakka, J.S. Rao, Promoter methylation and silencing of the tissue factor pathway inhibitor-2 (TFPI-2), a gene encoding an inhibitor of matrix metalloproteinases in human glioma cells, *Oncogene* 22 (29) (2003) 4509–4516.
- [61] H.V. de Silva, J.A.K. Harmony, W.D. Stuart, C.M. Gil, J. Robbins, Apolipoprotein J: structure and tissue distribution, *Biochemistry* 29 (1990) 5380–5389.
- [62] M. Khanna, K.N. Qin, R.W. Wang, K.C. Cheng, Substrate specificity, gene structure, and tissue-specific distribution of multiple human 3- α -hydroxysteroid dehydrogenases, *J. Biol. Chem.* 270 (1995) 20162–20168.
- [63] F. Galbiati, D. Volonte, O. Gil, G. Zanazzi, J.L. Salzer, M. Sargiacomo, P.E. Scherer, J.A. Engelman, A. Schlegel, M. Parenti, T. Okamoto, M.P. Lisanti, Expression of caveolin-1 and-2 in differentiating PC12 cells and dorsal root ganglion neurons: caveolin-2 is up-regulated in response to cell injury, *Proc. Natl. Acad. Sci. U. S. A.* 95 (17) (1998) 10257–10262.
- [64] T. Rich, P. Chen, F. Furman, N. Huynh, M.A. Israel, RTVP-1, a novel human gene with sequence similarity to genes of diverse species, is expressed in tumor cell lines of glial but not neuronal origin, *Gene* 180 (1–2) (1996) 125–130.
- [65] I. Song, C.Z. Chuang, R.C. Bateman Jr., Molecular cloning, sequence analysis and expression of human pituitary glutamyl cyclase, *J. Mol. Endocrinol.* 13 (1994) 77–86.
- [66] L.D. Griffin, W. Gong, L. Verot, S.H. Mellon, Niemann–Pick type C disease involves disrupted neurosteroidogenesis and responds to allopregnanolone, *Nat. Med.* 10 (7) (2004) 704–711.
- [67] S. Mellon, W. Gong, L.D. Griffin, Niemann pick type C disease as a model for defects in neurosteroidogenesis, *Endocr. Res.* 30 (4) (2004 Nov) 727–735.
- [68] D.S. Reddy, Role of neurosteroids in catamenial epilepsy, *Epilepsy Res.* 62 (2–3) (2004) 99–118.
- [69] F.W. Pfrieger, Role of cholesterol in synapse formation and function, *Biochim. Biophys. Acta* 1610 (2) (2003) 271–280.
- [70] A.R. Koudinov, N.V. Koudinova, Cholesterol homeostasis failure as a unifying cause of synaptic degeneration, *J. Neurol. Sci.* 229–230 (2005) 233–240.